Hindawi
Advances in Civil Engineering
Volume 2019, Article ID 3891080, 13 pages
https://doi.org/10.1155/2019/3891080

Research Article

Numerical Simulation of Parameters Optimization for Goaf Gas Boreholes

Jiajia Liu,[1,2,3,4] **Jianliang Gao**,[1,2,4] **Ming Yang**,[1,2,4] **Dan Wang**,[1] **and Liang Wang**[1]

[1]*State Key Laboratory Cultivation Base for Gas Geology and Gas Control, Henan Polytechnic University, Jiaozuo 454003, China*
[2]*School of Safety Science and Engineering, Henan Polytechnic University, Jiaozuo 454003, China*
[3]*Hunan Key Lab of Coal Safety Mining Technology, Hunan University of Science and Technology, Xiangtan 411201, China*
[4]*The Collaborative Innovation Center of Coal Safety Production of Henan Province, Jiaozuo 454003, China*

Correspondence should be addressed to Jiajia Liu; liujiajia@hpu.edu.cn and Ming Yang; yming@hpu.edu.cn

Received 19 August 2018; Accepted 12 December 2018; Published 10 January 2019

Guest Editor: Jian Sun

In view of the ground drilling of the N2206 working face in Shanxi Wangzhuang Coal Mine, the gas concentration is low and the extraction effect is not good. Fluent computational fluid dynamics software was used to simulate the ground extraction drilling position of the N2206 working face in the goaf (the distance from the top of the coal seam and the distance from the return to the wind). The numerical simulation results show that when the final hole of the ground extraction hole in the goaf is 16 m from the roof of the coal seam and the distance from the return air is 45 m, the extraction effect is optimal. The average extraction gas volume is 9.78 m^3/min, and the average extraction gas concentration is 43.95%, the best extraction effect is obtained. After optimizing the ground drilling position in the goaf and combining with the site implementation, the maximum gas scouring amount of the extraction is 12.59 m^3/min, which is 3.42 m^3/min higher than the original. The maximum gas concentration of extraction was 63.54%, which was 28.82% higher than the original. After optimization, the gas concentration of the extraction is more than 30%, and the extraction effect is very good. Field application results further validate the reliability of theoretical analysis and numerical simulation results.

1. Introduction

With the increasing coal mining depth in recent years, the gas pressure and content of coal seam increase obviously. Gas disaster has gradually become the primary problem that restricts the safe production of coal mine. The most universal technique to control gas disaster is gas extraction, which has two kinds: extraction by roadway and boreholes [1–3]. In this paper, we focus on the boreholes drilled from ground.

America was the first country that achieved success in exploiting coalbed methane resources by extracting gas with boreholes drilled from ground. In Australia, vertical borehole was the most common way to extract gas in goaf. Germany exploited coalbed methane resources from Ruhr coal field by boreholes drilled from ground in 1992. In most parts of China, low permeability, low saturation, and low reservoir pressure are the three characteristics of coal seam, which means it is hard to extract gas from the coal. We have drilled 40 ground boreholes in JiaoZuo and YangQuan since 1970 and carried out measures of hydraulic fracturing. Then, we conducted experimental studies of gas extracted from ground boreholes and underground drills in KaiLuan and TieFa coal fields with the help of United Nations Development Program. We have made some achievements on gas extraction by the method of ground boreholes in JinCheng and HuaiNan coal fields in China [4–6].

In the deep part of goaf, gas concentrating for a long time, the content of methane gas is much more than that in working face. The gas from goaf is one of the main sources of gas to working face. Extracting gas by boreholes drilled to goaf from ground is a main method to handle gas problem. There is a large body of work that has been done to investigate ground boreholes. Li et al analyzed the effect of gas extracted from ground boreholes in Jin Cheng field [7]. Li

et al studied the influential factors on gas extraction by ground boreholes and proposed an approach to enhance the efficiency of gas extraction [8]. Many foreign scholars have done a lot of research about gas disaster prevention, gas drainage in coal mine goaf, etc [9–16]. Many other scholars have also examined the effects of ground boreholes [17–20].

However, there are controversies about this question: whether the location of boreholes is a critical factor for gas extraction technique. Some scholars even hold opinion that the effect of the location can be neglected [21, 22]. Further research on the effect of the location of ground boreholes to the effect of gas extraction needs to be done to reach better effect. Based on the physical parameters of N2206 working face in WangZhuang mine in ShanXi Province, this paper investigates the poor efficiency of ground boreholes 1# and 2# drilled to goaf of N2206 working face by software Fluent to confirm the best location of ground boreholes.

2. The Theory of Gas Extraction from Ground Drilling to Gob

Gas extraction from goaf by ground boreholes does not have a long history in coal mining industry, whereas mines in America and Australia have made achievements of ground boreholes. The principle of gas extraction from ground drilling to gob is that as the following: the overlying rock above goaf can be divided into three vertical zones, including caved zone, fractured zone, and bended zone due to the influence of coal mining. As the working face advancing, there are many separations and fractures in the bended zone, largely enhancing the permeability of coal seam. Gas migration is much easier in the separations and fractures. Then, the ground boreholes are drilled into the bended zone to exact gas, reducing the thread of gas. Figure 1 shows the layout of ground boreholes to goaf.

3. The General Situation of Working Face and Numerical Simulation

3.1. The General Situation of N2206 Working Face. The strike length of tape roadway in N2206 is 2252 m; the strike length of intake air roadway is 2260 m; and the strike length of return air roadway is 2257 m. The inclination length of N2206 working face is 285 m. Figure 2 shows the sketch map of the N2206 working face. The yearly output of N2206 working face is 1.4MT with recovery ratio of 93%. The average thickness of coal seam is 5.99 m; the unit weight of coal is 1.4 t/m^3. The absolute gas emission rate is 76.5 m^3/min. Herein air flow counts for 32.2 m^3/min, and extracted gas counts for 44.3 m^3/min.

In the design, the ventilation in the N2206 working face is doubled. The inlet air roadway and tape roadway are filled with fresh air, and in the return air roadway and gas tail roadway is dirty air, i.e., two-intake and two-return. And then it is changed into three-intake and one-return. The inlet air roadway, tape roadway, and the return air are filled with fresh air, and the gas tail roadway is filled with dirty air [23].

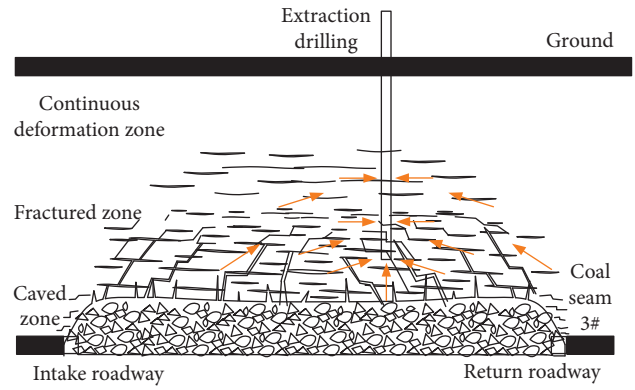

Figure 1: Arrangement plan about ground extraction drilling to gob.

3.2. Theoretical Calculation on the Height of Three Vertical Zones

(1) The theoretical formula of height to caved zone:

$$H_m = \frac{h}{(k-1)\cos\alpha}, \quad (1)$$

where h is the mining height, k is the average bulking coefficient of caved rock, and α is the dip of coal seam.

(2) The theoretical height of fractured zone:

$$H_l = \frac{100h}{ah+b} \pm c, \quad (2)$$

where a, b, and c are the undetermined coefficients: they are determined by the "Design code of coal mine" of Wangzhuang mine, shown in Table 1.

(3) The bended zone is stratum that starts from the upper boundary of fractured zone to earth surface, and we do not consider the bended zone in this paper because the sinking variation is small extremely. According to the relating materials of the N2206 working face, the overburden rock is medium hard rock mainly, the roof of N2206 working face is mixed with post stone and mudstone, and the floor is siltstone and mudstone. Figure 3 shows the histogram of coal-rock strata about N2206 working face. The working face follows strike longwall and takes caving coal mining for fully mechanized. The included angle of mining layer and the horizontal direction is 6° or so. The bulking coefficient of caved rock and roof coal are 1.26 and 1.3. The average theoretical height to caved zone and fractured zone is 14.6 m and 45.5 m based on the calculation formulas (1) and (2). We can calculate the thickness of left coal in gob which is 0.6 m based on the average thickness of coal seam, the recovery ratio, and the bulking coefficient of roof coal [24].

3.3. Physical Model of Gob. The width and height of intake roadway of N2206 working face are 5 m and 4 m; the width

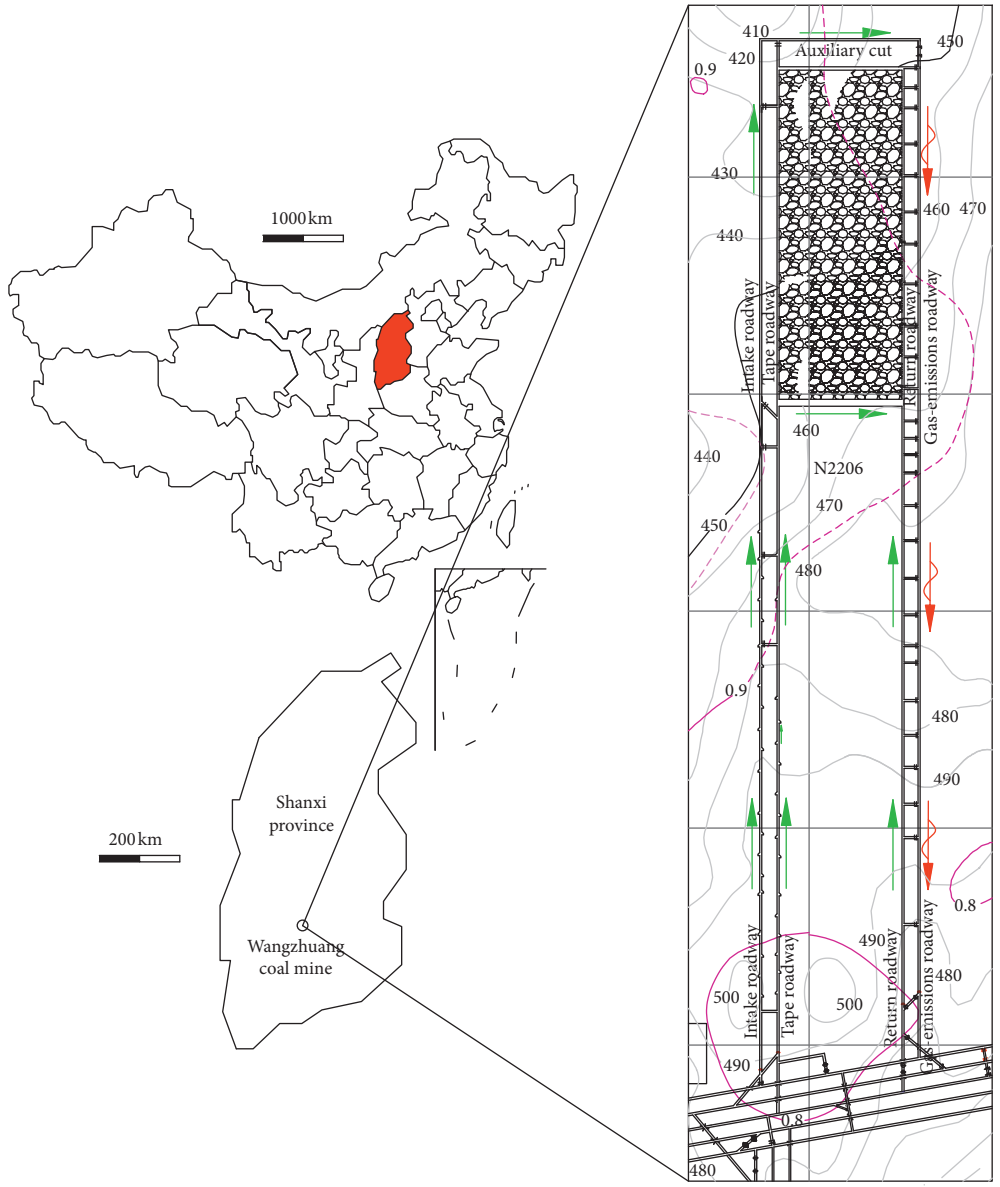

Figure 2: Arrangement plan of N2206 working face.

Table 1: Value table of undetermined constants a, b, and c.

Lithology	a	b	c
Hard rock	1.2	2.0	8.9
Medium hard rock	1.6	3.6	5.6
Soft rocks	3.1	5.0	4.0
Top soft rocks	5.0	8.0	3.0

and height of return roadway are 5 m and 4 m; the inclination and strike length of the working face are 285 m and 300 m; the length of intake roadway, tape roadway, and return roadway is all 20 m. The thickness of left coal in gob is 0.6 m, and the height of caved zone and fractured zone is 14.6 m and 45.5 m. The effect of goaf on the gas flowing regulation in gob can be neglected in the reason of the sinking variation which is small extremely in the three zones. This model neglected the bended zone, and the physical model is shown in Figure 4.

3.4. Mathematical Model of Gob

3.4.1. Hypothesis

(1) Taking the working zone is turbulent flow zone, and the laminar flow is the main flow state of gas flow in gob.

(2) We regard the porous media in gob as an isotropous area, and its permeability is constant in the reason of the randomness of the caved rock and the left coal.

Thickness (m)	Depth (m)	Histogram	Lithology
1.12	483.08		Mudstone
1.20	484.28		Sandstone
2.89	487.17		Siltstone
3.22	490.39		Natural coke
2.16	492.55		Siltstone
7.26	499.81		Sandstone
5.99	505.80		3# Coal seam
6.30	512.10		Siltstone
4.95	517.05		Mudstone
3.01	520.06		Siltstone
2.33	522.39		Sandstone
2.38	524.77		Aluminum mudstone
1.41	526.18		Mudstone
2.81	528.99		Sandstone
1.75	530.74		Siltstone
3.35	534.09		Mudstone
2.13	536.22		Siltstone
4.46	540.68		Mudstone
6.35	547.03		Siltstone
3.12	550.15		Mudstone
0.35	550.50		4# Coal seam
0.48	550.98		Mudstone
2.85	553.83		Sandstone
3.60	557.43		Mudstone
1.62	559.05		Sandstone
3.78	562.83		Sandy mudstone

Figure 3: Histogram of N2206 working face.

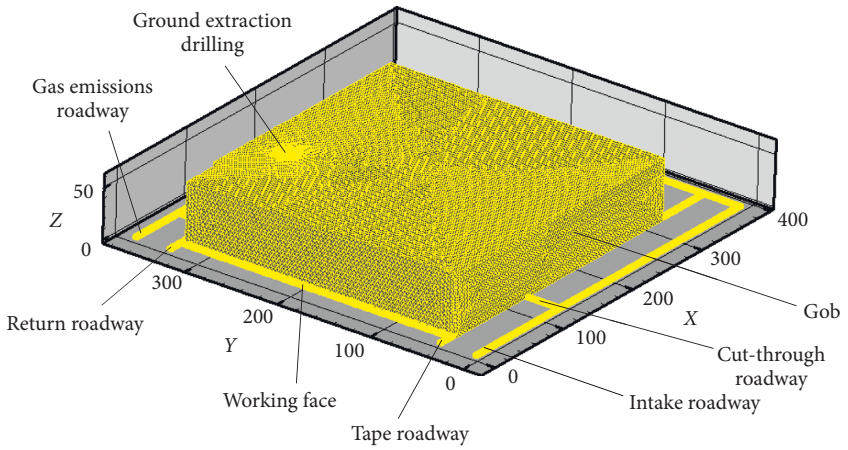

Figure 4: Physical model of gob to N2206 working face.

(3) Taking into account the gob gas is incompressible gas; we do not take into account the work of fluid viscosity caused by heat dissipation. We assumed the gas flow is steady and the process remains at a constant temperature.

(4) Ignoring the small component gases such as water vapor and nitrogen dioxide and assuming that the diffusion coefficient of the gas remains constant, the gas in the component transport is set to a mixed gas of methane, nitrogen, and oxygen.

3.4.2. Mathematical Model. The mathematical model of porous media in gob is as the following [25]:

(1) The mass conservation equation:

$$\frac{\partial (nu)}{\partial x} + \frac{\partial (nv)}{\partial y} + \frac{\partial (nw)}{\partial z} = S_{\mathrm{m}}. \tag{3}$$

(2) The momentum equation (Navier–Stokes):

$$\begin{aligned}
&\frac{\partial (n\rho uu)}{\partial x} + \frac{\partial (n\rho uv)}{\partial y} + \frac{\partial (n\rho uw)}{\partial z} = \frac{\partial}{\partial x}\left(n\mu \frac{\partial u}{\partial x}\right) \\
&\quad + \frac{\partial}{\partial y}\left(n\mu \frac{\partial u}{\partial y}\right) + \frac{\partial}{\partial z}\left(n\mu \frac{\partial u}{\partial z}\right) - n\frac{\partial P}{\partial x} + F_x, \\
&\frac{\partial (n\rho vu)}{\partial x} + \frac{\partial (n\rho vv)}{\partial y} + \frac{\partial (n\rho vw)}{\partial z} = \frac{\partial}{\partial x}\left(n\mu \frac{\partial v}{\partial x}\right) \\
&\quad + \frac{\partial}{\partial y}\left(n\mu \frac{\partial v}{\partial y}\right) + \frac{\partial}{\partial z}\left(n\mu \frac{\partial v}{\partial z}\right) - n\frac{\partial P}{\partial y} + F_y, \\
&\frac{\partial (n\rho wu)}{\partial x} + \frac{\partial (n\rho wv)}{\partial y} + \frac{\partial (n\rho ww)}{\partial z} = \frac{\partial}{\partial x}\left(n\mu \frac{\partial w}{\partial x}\right) \\
&\quad + \frac{\partial}{\partial y}\left(n\mu \frac{\partial w}{\partial y}\right) + \frac{\partial}{\partial z}\left(n\mu \frac{\partial w}{\partial z}\right) - n\frac{\partial P}{\partial z} + F_z.
\end{aligned} \tag{4}$$

(3) The component transport equation:

$$\begin{aligned}
&\frac{\partial (\rho c_{\mathrm{s}} u)}{\partial x} + \frac{\partial (\rho c_{\mathrm{s}} v)}{\partial y} + \frac{\partial (\rho c_{\mathrm{s}} w)}{\partial z} = \frac{\partial}{\partial x}\left(D_s \frac{\partial \rho c_{\mathrm{s}}}{\partial y}\right) \\
&\quad + \frac{\partial}{\partial y}\left(D_s \frac{\partial \rho c_{\mathrm{s}}}{\partial y}\right) + \frac{\partial}{\partial z}\left(D_s \frac{\partial \rho c_{\mathrm{s}}}{\partial z}\right) + S_{\mathrm{s}},
\end{aligned} \tag{5}$$

where u, v, and w are velocity components of the directions x, y, and z; n is the porosity; S_{m} is the source item of mass; ρ is the density of gas in gob; μ is the dynamic viscosity of air; F_x, F_y, and F_z are the mass force component on microunit in every direction; C_{s} is the volume concentration of component S; S_{s} is the productivity of component; ρC_{s} is the mass concentration of component; and D_{s} is the diffusion coefficient of the component.

The turbulence model of the working face is realizable $k-\varepsilon$:

$$\begin{aligned}
&\frac{\partial (\rho ku)}{\partial x} + \frac{\partial (\rho kv)}{\partial y} + \frac{\partial (\rho kw)}{\partial z} = \frac{\partial}{\partial x_j} \\
&\quad \cdot \left[\left(\mu + \frac{\mu_t}{\sigma x_j}\right)\frac{\partial k}{\partial x_j}\right] + G_k - \rho\varepsilon - Y_{\mathrm{M}}, \\
&\frac{\partial (\rho\varepsilon u)}{\partial x} + \frac{\partial (\rho\varepsilon v)}{\partial y} + \frac{\partial (\rho\varepsilon w)}{\partial z} = \frac{\partial}{\partial x_j} \\
&\quad \cdot \left[\left(\mu + \frac{\mu_t}{\sigma_\varepsilon}\right)\frac{\partial \varepsilon}{\partial x_j}\right] + \rho C_1 E\varepsilon \\
&\quad - \rho C_2 \frac{\varepsilon^2}{k + \sqrt{\nu\varepsilon}} + C_{1\varepsilon}\frac{\varepsilon}{k} C_{3\varepsilon} G_b,
\end{aligned} \tag{6}$$

where G_k is the generation item of turbulence energy caused by the average velocity of gas; G_b is the generation item of turbulence energy caused by buoyancy, which is 0 to the incompressible fluid; Y_{M} is the contribution of pulse expansion caused by the turbulence flow to the compressible fluid; where $C_{1\varepsilon} = 1.44, C_2 = 1.9, C_{3\varepsilon} = 0, \sigma_\varepsilon = 1.0, \mu_{\mathrm{t}} = \rho C_\mu (k^2/\varepsilon)$.

3.5. The Boundary Conditions and Numerical Simulation Process

3.5.1. Boundary Conditions. The intake roadway of working face is velocity-inlet, the average velocity of tape roadway, return air roadway and inlet air roadway are, respectively, 2.6 m/s, 1.1 m/s, and 1.6 m/s. The volume fraction of O_2 and CH_4 are, respectively, 21% and 0% in the intake roadway. The gas emissions roadway was set as out-flow; the working face and goaf of solid wall are set as nonslip boundary condition, which is $u = v = w = 0$; the juncture of working face and goaf is set as the interior boundary. Detailed boundary conditions and parameters are shown in Table 2. The permeability of goaf presents continuous distribution as "O" because of the support effect of surrounding rock in gob. Using C language, the gas emission intensity of goaf and goaf permeability are defined as the continuous distribution of the custom function.

3.5.2. The Numerical Simulation Process. The modeling tool Gambit is used to construct the physical model in the Cartesian coordinate system and unstructured meshing. Fluent software is used for numerical simulation solution, and finally, the simulation results into Tecplot for postprocessing operation. The control equation is discreted in the method of control volume, among which the format convection term and diffusion term are in the format of Quick. The iteration calculation was accomplished in combination of relaxing factor and tridiagonal-matrix algorithm. The coupling of pressure-velocity takes simple arithmetic [26].

Table 2: Boundary conditions and parameters.

Location/name	Boundary conditions	Parameters values
Tape roadway	Velocity-inlet	2.6 m/s
Return air roadway	Velocity-inlet	1.1 m/s
Inlet air roadway	Velocity-inlet	1.6 m/s
Gas emissions roadway	Out-flow	/
Intake roadway	O_2 respectively	21%
Intake roadway	CH_4 respectively	0%
Working face solid wall	Nonslip boundary	$u = v = w = 0$
Goaf solid wall	Nonslip boundary	$u = v = w = 0$
Juncture of working face and goaf	Interior boundary	/
Permeability of goaf	"O" distribution	/

4. The Result Analysis of Numerical Simulation Process on Gob

From the documents, it is reasonable to layout gas extraction drilling in the roof of the caved zone and the lower-middle part of the fractured zone. There would appear series questions about gas extraction difficulties and low quantity of gas extraction if the layout position is too high. If the layout is in the lower level, it is possible to communicate directly with the cave zone, and there would be drainage of large flow, its composition is mainly air leakage problem of goaf etc. If the layout position is near the return air roadway, the return air roadway would be linked up through fractures, and the main component of the gas extraction is air. Since the return air roadway is near the high concentration area of the goaf, if the layout position of the drilling is far from the return air roadway, there will be problems such as lower gas concentration and lower flow rate. Thus, the reasonable layout parameters are crucial to the effect of gas extraction. Now, we should combine the existing questions of gas extraction drilling from ground to gob of 1#, 2# on N2206 working face and numerical simulation to optimize the layout parameters. The gas is collected to the circle of "O" through seepage after gas desorption around the coal-rock based on the theory of circle "O" about fracture distribution in overlaying rock. To achieve the long gas extraction time, the big zone of gas extraction, and the high gas drainage efficiency, the gas extraction drilling should be placed to the inner of circle "O".

4.1. Optimization of the Vertical Gas Extraction Height from Ground to Gob. Based on the experience of 1 # and 2 # mining ground drilled holes, the range of the hole location of the borehole drilling is estimated on the basis of grasping the inclination of the coal seam and so on. When the horizontal distance is 45 m, the numerical simulation software is used to simulate the drilling position of the vertical extraction of 10 m, 16 m, and 22 m from the roof of the coal seam. The simulation results are shown in Figures 5 and 6.

From Figures 5 and 6, the distribution trends of gas in gob are approximately same when the vertical height of gas extraction drills is selected as 10 m, 16 m, and 22 m. The deeper the gob, the higher the concentration of the gas in the horizontal direction of gob. In the vertical direction, the concentration of gas upside the gob is bigger than the downside because of the effect of gas buoyancy. For the distributional profile of gas in gob of $Y = 50$ m and $Y = 290$ m, the scope of gas concentration of 5% in gob is 129 m and 130 m, which is relevant with the vertical height of gas extraction drilling, when the figure is 10 m. The scope of gas concentration of 5% in gob is 138 m and 140 m, which is relevant with the vertical height of gas extraction drilling, when the figure is 16 m and the scope is the widest with low gas concentration. By contrast, when the scope of gas concentration of 5% in gob is 99 m and 112 m, the figure is 22 m and the scope is the narrowest with low gas concentration. For the distributional planar graph of gas in gob of $Z = 1$ m and $Z = 20$ m, the scope of gas concentration of 5% in gob is 121 m and 122 m, which is relevant with the vertical height of gas extraction drilling, when the figure is 10 m near the side of belt crossheading. The scope of gas concentration of 5% in gob is 129 m and 134 m, which is relevant with the vertical height of gas extraction drilling, when the figure is 16 m and the scope was the widest with low gas concentration. The scope of gas concentration of 5% in gob is 108 m and 109 m, which is relevant with the vertical height of gas extraction drilling, when the figure is 22 m and the scope was the narrowest with low gas concentration. Analyzing the distributional profile and planar graph of gas in gob, we found that the scope of low gas concentration in gob is the widest, and the scope of high gas concentration in gob is the narrowest with the vertical height of gas extraction drilling is 16 m. The overall effect of gas extraction is best.

4.2. The Optimization of Horizontal Position on Drilling of Ground Gas Extraction to Gob. We performed numerical simulation by Fluent software with the horizontal distance between the end drilling and the return air roadway of 35 m, 45 m, and 55 m based on the decided vertical height of gas extraction from ground of 16 m. Figures 7 and 8 show the simulation results.

From Figures 7 and 8, the distribution trends of gas in gob are approximately same when the horizontal distance of gas extraction drillings is selected as 35 m, 45 m, and 55 m. The closer to the depth of the gob, the higher the concentration of gas in the strike direction of the gob. In the vertical direction, the concentration of gas upside the gob is bigger than the downside because of the effect of gas buoyancy. For the distributional profile of gas in gob of $Y = 50$ m and $Y = 290$ m, the scope of gas concentration of 5% in gob is 112 m and 99 m,

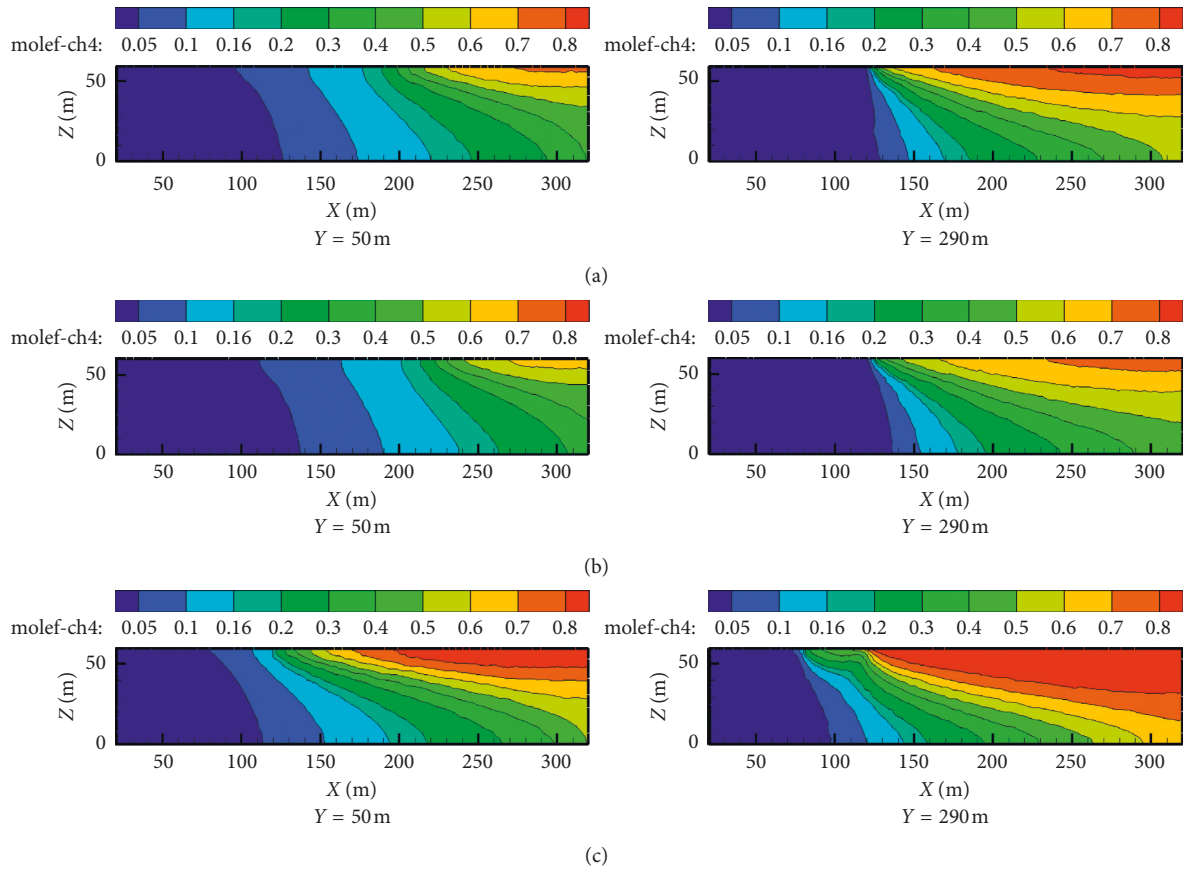

Figure 5: Distributional profile of gas in gob with different vertical heights of ground gas extraction. (a) Horizontal distance is 45 m and vertical distance is 10 m. (b) Horizontal distance is 45 m and vertical distance is 16 m. (c) Horizontal distance is 45 m and vertical distance is 22 m.

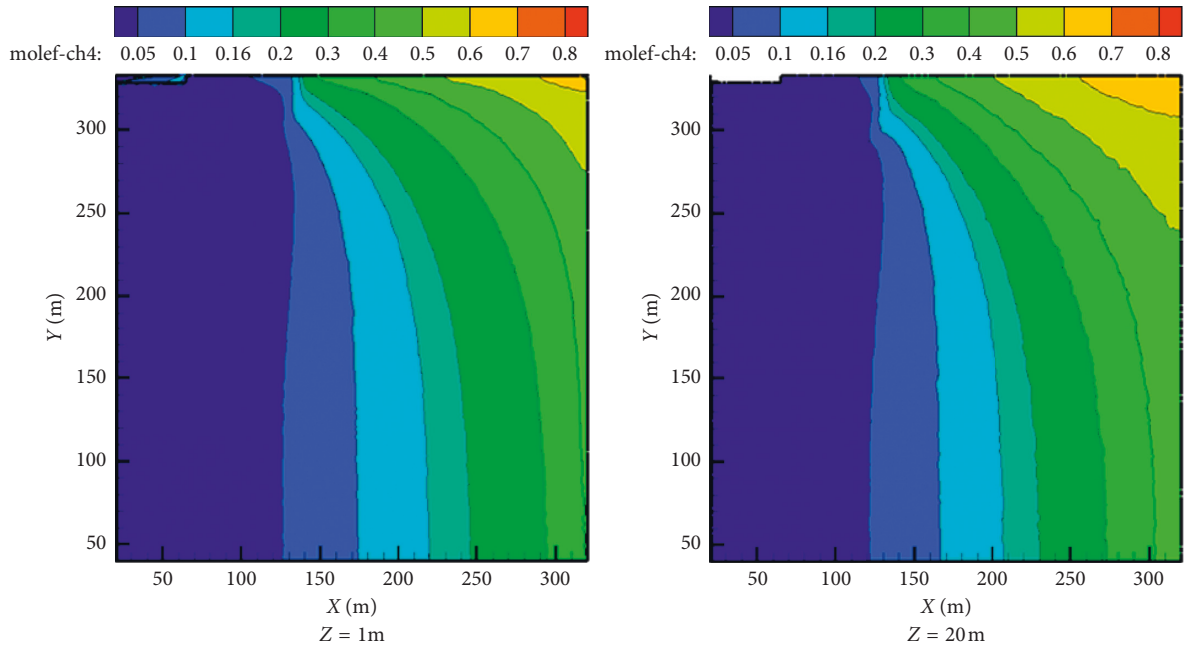

Figure 6: Continued.

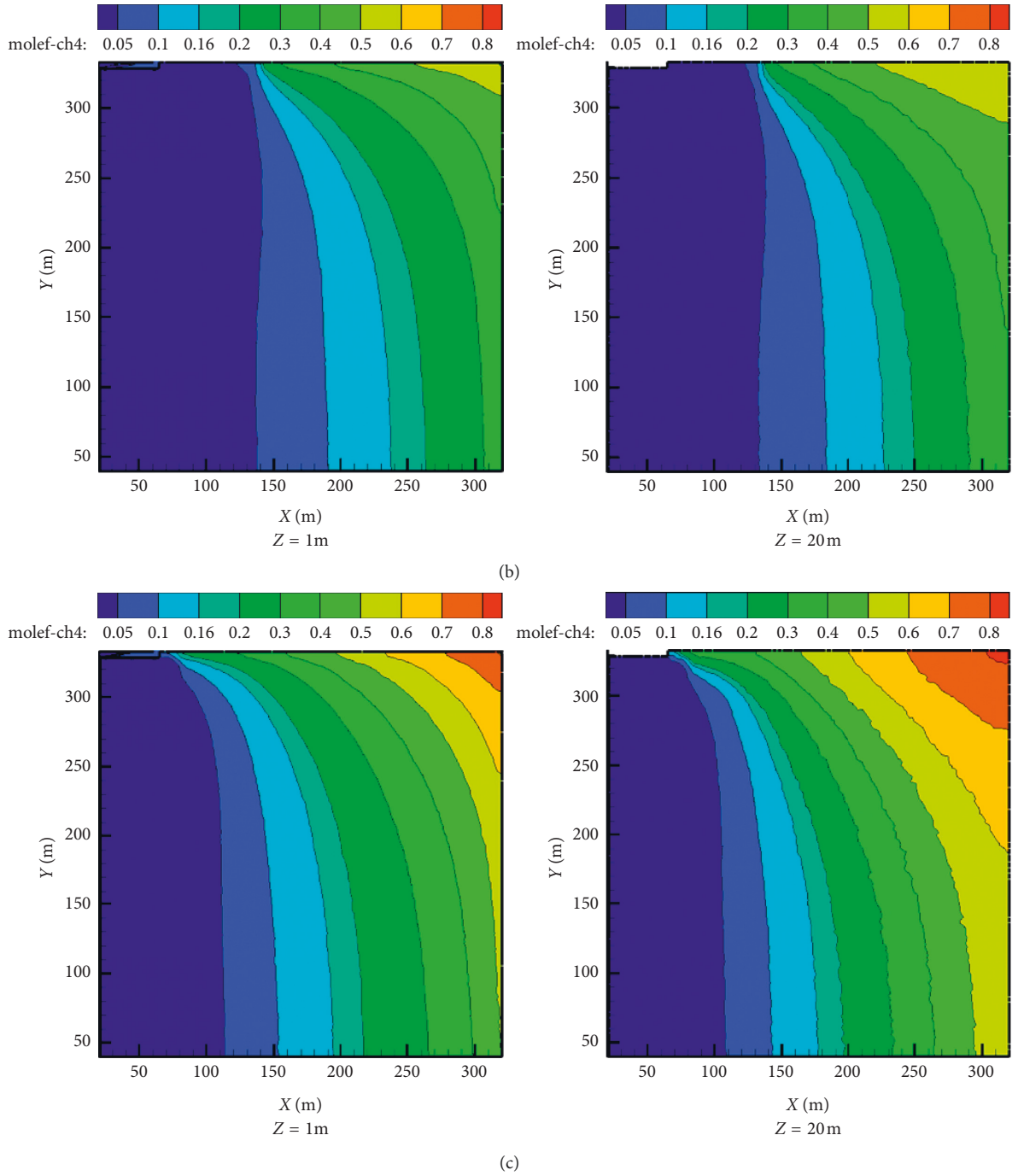

Figure 6: Distributional planar graph of gas in gob with different vertical heights of ground gas extraction. (a) Horizontal distance is 45 m and vertical distance is 10 m. (b) Horizontal distance is 45 m and vertical distance is 16 m. (c) Horizontal distance is 45 m and vertical distance is 22 m.

which is relevant with the horizontal distance of gas extraction drilling, when the figure is 35 m. The scope of gas concentration of 5% in gob is 140 m and 135 m, which is relevant with horizontal distance of gas extraction drilling, when the figure is 55 m and the scope was the widest with low gas concentration. The scope of gas concentration of 5% in gob is 111 m and 98 m, which is relevant with the horizontal distance of gas extraction drilling, when the figure is 55 m and the scope was the narrowest with low gas concentration. For the distributional planar graph of gas in gob of $Z = 1$ m and $Z = 20$ m, the scope of gas concentration of 5% in gob is 112 m and 108 m, which is relevant with the horizontal distance of gas extraction drilling, when the figure is 35 m near the side of belt crossheading. The scope of gas concentration of 5% in gob is 120 m and 132 m, which is relevant with the horizontal distance of gas extraction drilling, when the figure is 45 m, and the scope was widest with low gas concentration. The scope of gas concentration of 5% in gob is 110 m and 107 m, which is relevant with the vertical

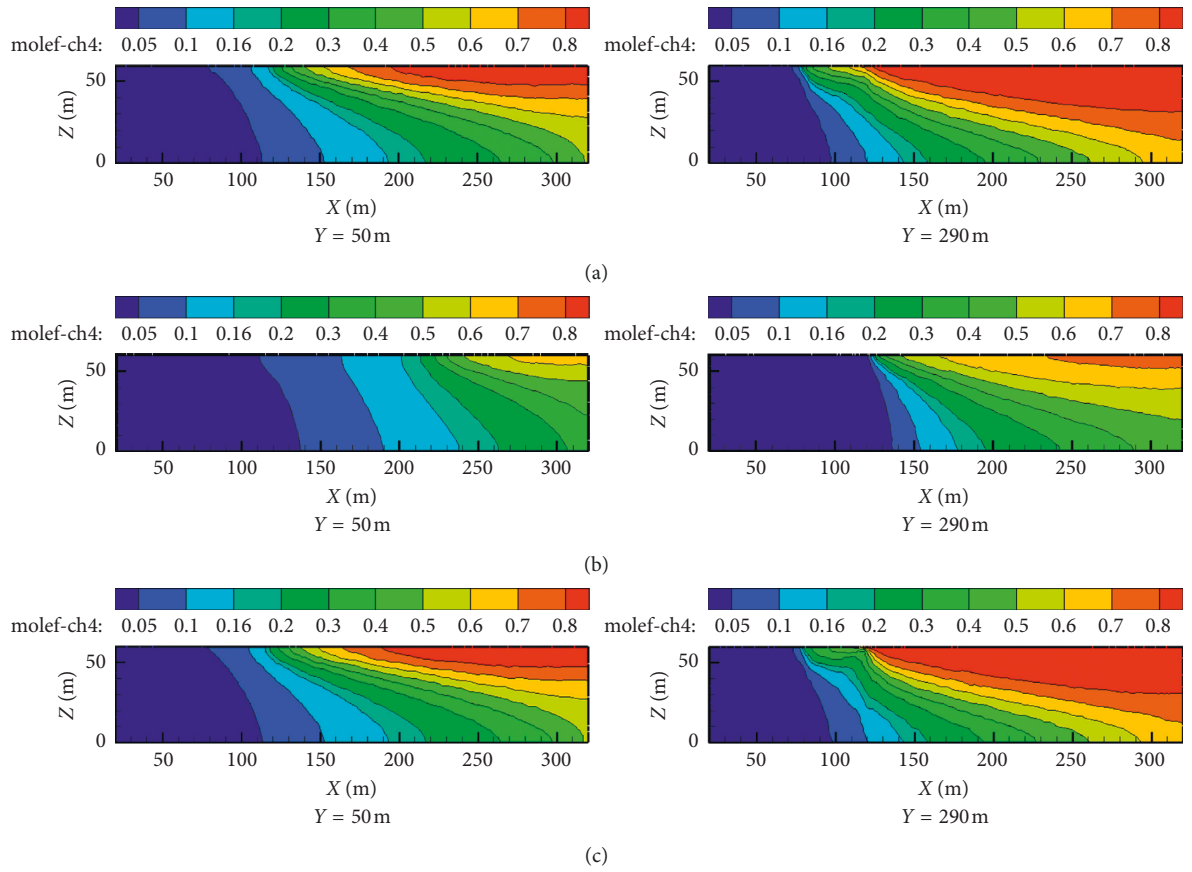

Figure 7: The distributional profile of gas in gob with different horizontal distances of ground gas extraction. (a) Horizontal distance is 35 m and vertical distance is 16 m. (b) Horizontal distance is 45 m and vertical distance is 16 m. (c) Horizontal distance is 55 m and vertical distance is 16 m.

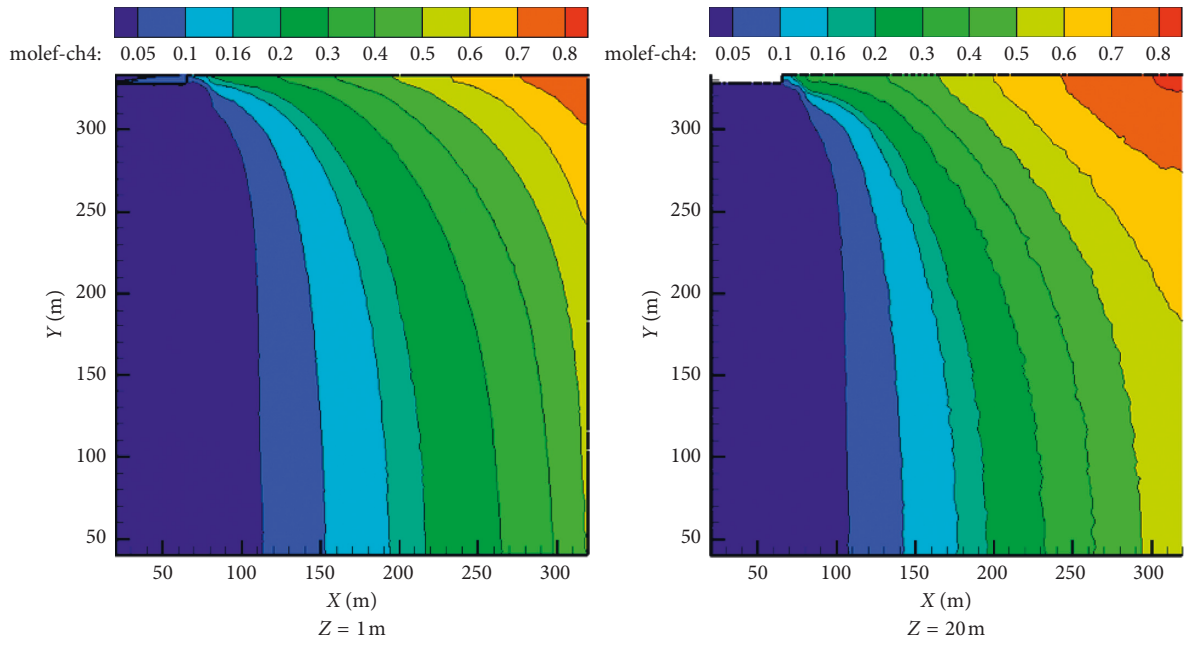

Figure 8: Continued.

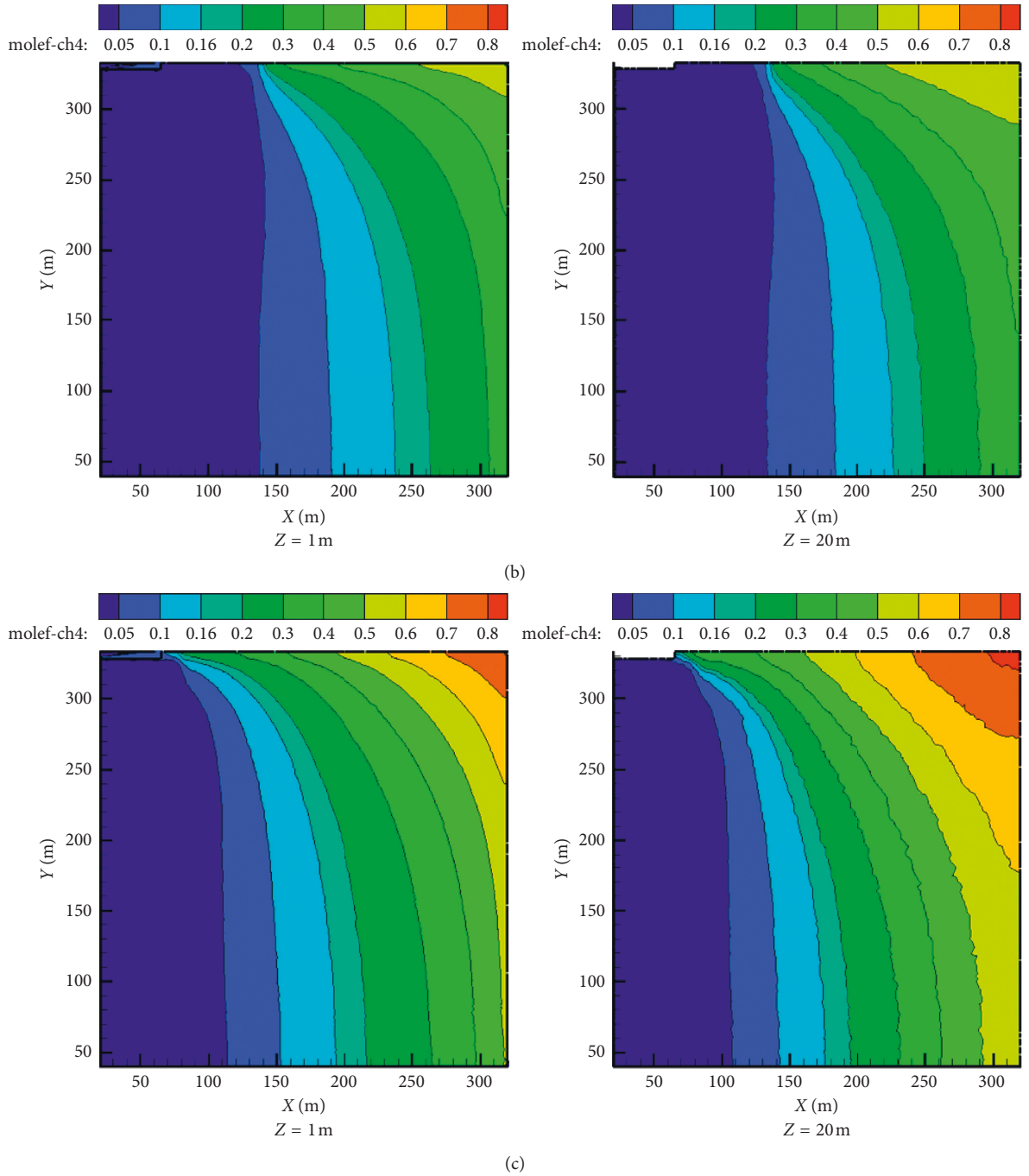

Figure 8: Distributional planar graph of gas in gob with different horizontal distances of ground gas extraction. (a) Horizontal distance is 35 m and vertical distance is 16 m. (b) Horizontal distance is 45 m and vertical distance is 16 m. (c) Horizontal distance is 55 m and vertical distance is 16 m.

horizontal distance of gas extraction drilling, when the figure is 55 m, and the scope was the narrowest with low gas concentration. Right now, the distance between the end drilling and the return air roadway was too far; thus, it is not in the "O" zone of fracture development and results in the nonideal gas extraction effect. Analyzing the distributional profile and concentration in gob was the widest and the high gas concentration is near the deep of the gob with the horizontal distance of gas extraction drilling, when the figure is 45 m. The overall effect of gas extraction is best.

To verify the best gas extraction location about ground drilling, we monitored the ground drilling with different vertical heights and horizontal distances and simulated and solved the condition of gas extraction with different vertical heights and horizontal distances by combining the in situ data as shown in Table 3.

From Table 3, the gas extraction effect is obviously different with different vertical heights and horizontal distances. When the horizontal distance of ground drilling is 45 m, the vertical height is set as 10 m, 16 m, and 22 m, the

Table 3: Gas extraction effect under different vertical height and horizontal distance.

Location	Average pure quantity of gas extraction (m^3/min)	Average mixture quantity of gas extraction (m^3/min)	Average concentration of gas extraction (%)
(45 m, 10 m)	5.22	19.6	26.63
(45 m, 16 m)	9.78	22.2	43.95
(45 m, 22 m)	4.79	23.3	20.56
(35 m, 16 m)	4.54	26.4	9.71
(55 m, 16 m)	4.32	18.1	23.87

average pure quantity and the average concentrations of gas extraction are 9.78 m^3/min and 43.95%, the vertical height is 16 m, and the effect of gas extraction is the best. When the vertical height of ground drilling is 16 m, the horizontal distance is set as 35 m, 45 m, and 55 m, among which the distance between the drilling and the return air roadway is near with the horizontal distance of 35 m. The main gas component of gas extraction is air, the mixture quantity of gas extraction is bigger, and the concentration of gas extraction is lower. Through monitoring the outlet flow rate, the mixture quantity of gas extraction is only 18.1 m^3/min because the distance between the end drilling and the return air roadway was too far; thus, it is not in the "O" zone of fracture development. The pure quantity and concentration of gas extraction are biggest with the horizontal distance of 45 m. In conclusion, the effect of gas extraction is the best with the 16 m vertical height and the 45 m horizontal distance.

5. In Situ Test

We gain that the best effect of gas extraction with the 16 m vertical height and the 45 m horizontal distance through theoretical analysis and numerical simulation on the low gas concentration question about the ground drilling 1# and 2# to N2206 working face in Wangzhuang coal mine. To give a further validation of the reliability of theoretical analysis and numerical simulation, we performed gas extraction from ground to gob with the optimized parameters. Figures 9 and 10 show the pure quantity and concentration of gas extraction before and after drilling optimization about 1# and 2#.

From Figures 9 and 10, when the pure quantity and concentration of gas extraction are low in 1# and 2#, the concentration of gas extraction from the drilling are both lower than 30%. The effect of gas extraction in 1# is the most nonideal with the concentration of gas extraction only 10% or so. After optimization, the pure quantity and concentration of gas extraction increased obviously. The maximum pure quantity of gas extraction is 12.59 m^3/min and have an increase of 3.42 m^3/min than before, the maximum concentration of gas extraction is 63.54% and have an increase about 28.82% than before and the concentration of gas extraction from the drilling is higher and over 30%. The effect of gas extraction is relatively ideal, and it verified the reliability of theoretical analysis and numerical simulation.

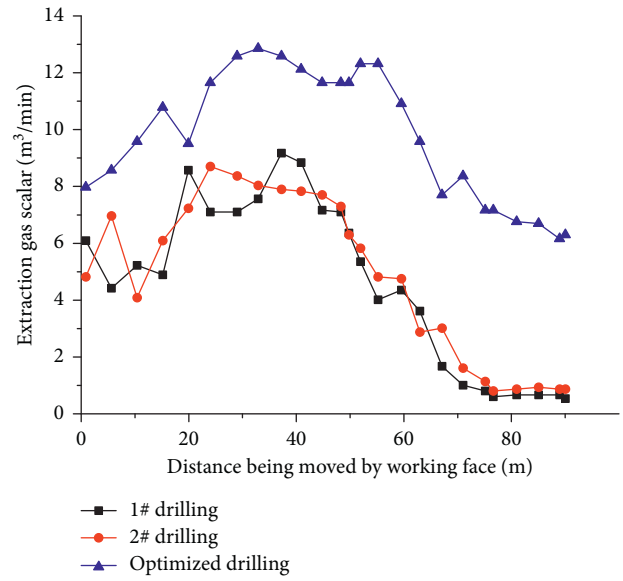

Figure 9: Correlation curve of pure quantity of gas extraction before and after the optimization of ground extraction drilling to gob.

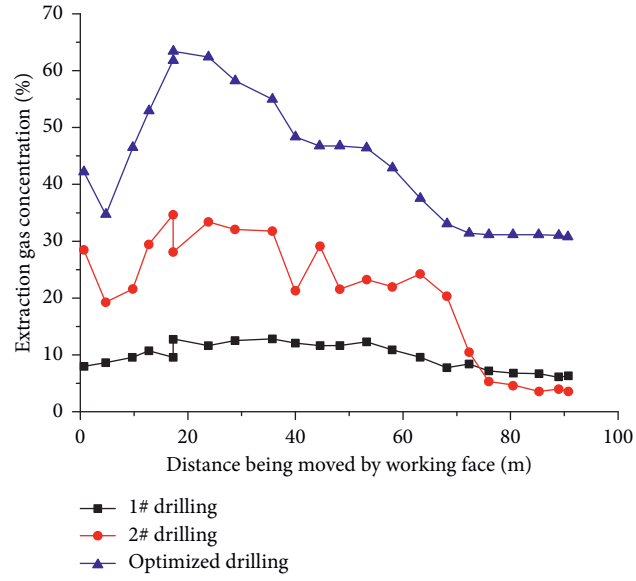

Figure 10: Correlation curve of concentration of gas extraction before and after the optimization of ground extraction drilling to gob.

6. Conclusions

(1) Theoretical analysis and numerical simulation show that it is obvious to see the range of low gas concentration is widest and the range of high gas concentration is narrowest when vertical height of ground extraction drilling of gob is 16 m and

horizontal distance is 45 m. In the deep of gob, the high gas concentration can be shown, and the ground drilling shows the optimum efficiency to the gas extraction. The in situ data and the monitoring simulation data show that it has the best extraction effect with 16 m vertical height and 45 m horizontal distance; under this condition, the average pure quantity and the average concentration of gas extraction are 9.78 m^3/min and 43.95%, respectively.

(2) After optimization, the pure quantity and concentration of gas extraction have an obvious increase. The maximum pure quantity of gas extraction is 12.59 m^3/min and has an increase of about 3.42 m^3/min than before; the maximum concentration of gas extraction is 63.54% and has an increase about 28.82%, and the concentration of gas extraction from the drilling is higher over 30%. The effect of gas extraction is more ideal. The theoretical analysis and numerical simulation have been proved.

Data Availability

The data used to support the findings of this study are available from the corresponding author upon request.

Disclosure

A very short abstract of this manuscript was presented as a poster at the International Conference on Coal Technology.

Conflicts of Interest

The authors declare that they have no conflicts of interest.

Acknowledgments

This study was supported by the National Natural Science Foundation of China (51604101, 51704099, and 51734007), funded by the Doctoral Fund of Henan Polytechnic University (no. B2018-59), State Key Laboratory Cultivation Base for Gas Geology and Gas Control (Henan Polytechnic University) (WS2017B06), supported by the Henan Postdoctoral Foundation, and Open Research Fund Program of Hunan Province Key Laboratory of Safe Mining Techniques Of Coal Mines (Hunan University of Science and Technology) (201502).

References

[1] B. Lin, F. Yan, C. Zhu et al., "Cross-borehole hydraulic slotting technique for preventing and controlling coal and gas outbursts during coal roadway excavation," *Journal of Natural Gas Science and Engineering*, vol. 26, pp. 518–525, 2015.

[2] H. Chen, Y. Cheng, T. Ren, H. Zhou, and Q. Liu, "Permeability distribution characteristics of protected coal seams during unloading of the coal body," *International Journal of Rock Mechanics and Mining Sciences*, vol. 71, no. 3, pp. 105–116, 2014.

[3] K. Wang, J. Zang, G. Wang, and A. Zhou, "Anisotropic permeability evolution of coal with effective stress variation and gas sorption: model development and analysis," *International Journal of Coal Geology*, vol. 130, pp. 53–65, 2014.

[4] Q. Liu and Y. Cheng, "Measurement of pressure drop in drainage boreholes and its effects on the performance of coal seam gas extraction: a case study in the Jiulishan Mine with strong coal and gas outburst dangers," *Natural Hazards*, vol. 71, no. 3, pp. 1475–1493, 2013.

[5] J. Liu, Z. Liu, J. Xue, K. Gao, and W. Zhou, "Application of deep borehole blasting on fully mechanized hard top-coal presplitting and gas extraction in the special thick seam," *International Journal of Mining Science and Technology*, vol. 25, no. 5, pp. 55–60, 2015.

[6] J. Fu, X. Fu, X. Hu, L. Chen, and J. Ou, "Research into comprehensive gas extraction technology of single coal seams with low permeability in the Jiaozuo coal mining area," *Mining Science and Technology (China)*, vol. 21, no. 4, pp. 483–489, 2011.

[7] G. Li, G. Li, and G. Liu, "Analysis on the ground extraction effect of coal-bed methane at typical area in Jincheng, China," *Journal of China Coal Society*, vol. 39, no. 9, pp. 1932–1937, 2014.

[8] R. Li, Y. Liang, J. Zhang et al., "Influencing factors to extraction efficiency of surface goaf hole," *Journal of China Coal Society*, vol. 34, no. 7, pp. 942–946, 2009.

[9] M. Jaszczuk and A. Pawlikowski, "A model of equilibrium conditions of roof rock mass giving consideration to the yielding capacity of powered supports," *Archives of Mining Sciences*, vol. 62, no. 4, pp. 689–704, 2017.

[10] W. Dziurzynski, A. Krach, and T. Palka, "Computer simulation of the propagation of heat in abandoned workings insulated with slurries and mineral substances," *Archives of Mining Sciences*, vol. 59, no. 1, pp. 3–23, 2014.

[11] S. A. Saki, J. F. Brune, G. E. Bogin, J.W. Grubb, M.Z. Emad, and R.C. Gilmore, "CFD study of the effect of face ventilation on CH4 in returns and explosive gas zones in progressively sealed longwall gobs," *Journal of the Southern African Institute of Mining and Metallurgy*, vol. 117, no. 3, pp. 257–262, 2017.

[12] S. J. Schatzel, R. B. Krog, and H. Dougherty, "Methane emissions and airflow patterns on a longwall face: potential influences from longwall gob permeability distributions on a bleederless longwall," *Transactions*, vol. 342, no. 1, pp. 51–61, 2017.

[13] J. Cygankiewicz, "Determination of critical conditions of spontaneous combustion of coal in longwall gob areas/wyznaczanie warunków krytycznych samozapalania węgla W zrobach scian," *Archives of Mining Sciences*, vol. 60, no. 3, pp. 761–776, 2015.

[14] C. Ö. Karacan and R. A. Olea, "Sequential Gaussian cosimulation of rate decline parameters of longwall gob gas ventholes," *International Journal of Rock Mechanics and Mining Sciences*, vol. 59, pp. 1–14, 2013.

[15] S. J. Schatzel, C. Ö. Karacan, H. Dougherty, and G. V. R. Goodman, "An analysis of reservoir conditions and responses in longwall panel overburden during mining and its effect on gob gas well performance," *Engineering Geology*, vol. 127, pp. 65–74, 2012.

[16] H. N. Dougherty, C. Özgen Karacan, and G. V. R. Goodman, "Reservoir diagnosis of longwall gobs through drawdown tests and decline curve analyses of gob gas venthole productions," *International Journal of Rock Mechanics and Mining Sciences*, vol. 47, no. 5, pp. 851–857, 2010.

[17] C. Ö. Karacan, "Analysis of gob gas venthole production performances for strata gas control in longwall mining,"

International Journal of Rock Mechanics and Mining Sciences, vol. 79, pp. 9–18, 2015.

[18] W. Qin, J. Xu, and G. Hu, "Optimization of abandoned gob methane drainage through well placement selection," *Journal of Natural Gas Science and Engineering*, vol. 25, pp. 148–158, 2015.

[19] H. Guo, C. Todhunter, Q. Qu, and Z. Qin, "Longwall horizontal gas drainage through goaf pressure control," *International Journal of Coal Geology*, vol. 150-151, pp. 276–286, 2015.

[20] B. Qu and H. Scott, "Effective goaf gas capture design at Ravensworth underground mine," *International Journal of Mining Science and Technology*, vol. 24, no. 3, pp. 379–383, 2014.

[21] T. Xia, F. Zhou, J. Liu, S. Hu, and Y. Liu, "A fully coupled coal deformation and compositional flow model for the control of the pre-mining coal seam gas extraction," *International Journal of Rock Mechanics and Mining Sciences*, vol. 72, pp. 138–148, 2014.

[22] J. G. Wang, J. Liu, and A. Kabir, "Combined effects of directional compaction, non-Darcy flow and anisotropic swelling on coal seam gas extraction," *International Journal of Coal Geology*, vol. 109-110, pp. 1–14, 2013.

[23] Y. Wu, J. Wu, J. Wang, and C. Zhou, "The law of gas distribution in goaf of fully mechanized top-coal caving working face with "double-U"ventilation system," *Journal of china coal society*, vol. 36, no. 10, pp. 1705–1708, 2011.

[24] H. Su, *Stability Control of Surrounding Rock in Gob-Side Entry Retain with Fully Mechanized Top Coal Caving and Technique of Gas Control*, China University of Mining and Technology, Beijing, China, 2015.

[25] K. Wang, S. Jiang, and W. Zhang, "Numerical simulation of tail roadway change to gas flow field in goaf," *Journal of Mining and Safety Engineering*, vol. 1, pp. 124–130, 2012.

[26] F. Wang, *Computational Fluid Dynamic Analyse*, Press of Tsing Hua University, Beijing, China, 2004.